J. Fluid Mech. (1983), *vol.* 126, *pp.* 59–73
Printed in Great Britain

Rarefaction shock wave near the critical liquid–vapour point

By A. A. BORISOV, AL. A. BORISOV, S. S. KUTATELADZE
AND V. E. NAKORYAKOV

Institute of Thermophysics, Siberian Branch of the USSR Academy of Sciences,
Novosibirsk-90, 630090, USSR

(Received 21 April 1981 and in revised form 19 April 1982)

The existence of a rarefaction shock wave or negative shock wave in a substance whose unperturbed state is close to the thermodynamic critical liquid–vapour point has been demonstrated experimentally. Its evolution and propagation velocity in a shock tube with Freon-13 as the test substance are described. It is shown that the steepness of the wave front does not diminish as the wave evolves. An equation is derived that describes the evolution of long-wave perturbations near the critical point.

1. Introduction

Phase transitions of the second kind and critical phenomena are among the most interesting unsolved problems of the physics of matter in the condensed state. At present the abnormal behaviour of the thermodynamic parameters, such as the infinite increase in the specific heats at constant pressure and volume and the resulting decrease in both the isothermal and adiabatic speeds of sound, the almost complete absence of diffusion in binary mixtures near the critical point, have been studied extensively.

The question of the dynamics of finite-amplitude perturbations of pressure, density and temperature in the critical region has not, however, been considered before in the literature. One should mention just one study devoted to shock waves near the critical point, namely that by Zeldovich (1946), who analysed the entropy condition for shock-wave stability and predicted theoretically the possible existence of rarefaction shock waves. The effect of the sign of $(\partial^2 P/\partial V^2)_S$ on the structure of compression and rarefaction waves was discussed by Thompson & Lambrakis (1973). Up until now no experiments have either supported or disproved Zeldovich's conjecture, probably because of the considerable difficulties involved in carrying out such an experiment.

In the present paper we describe the results of theoretical and experimental studies of the dynamics of negative shock waves in a substance whose unperturbed parameters are close to the thermodynamic critical point.

2. Experimental studies of rarefaction waves

To study substances in the critical region the following requirements should be met:

(i) the substance should be chemically pure;

(ii) the test volume should be maintained at a constant temperature with high accuracy (0·001 K) for a long period of time;

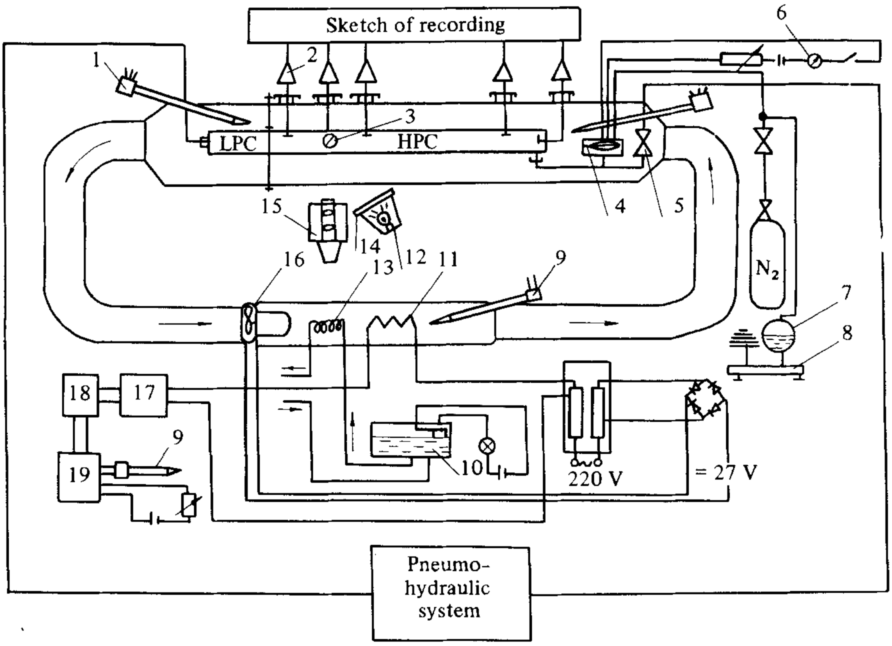

FIGURE 1. Schematic representation of experimental arrangement.

(iii) the probes for measuring the static and dynamic characteristics should be highly accurate.

Experimental studies of the structure of compression and rarefaction waves require a test section of considerable size. The maximum sizes of the cells that have been used so far for the measurement of the thermodynamic properties of substances close to the critical point have been no more than a few centimetres. Hence the mass of the substance studied has been a few tens of grams.

The main function of the specially designed experimental set-up (Kutateladze *et al.* 1980) shown in figure 1 is to ensure highly accurate temperature control along the shock tube, which consists of two sections, the high- and low-pressure chambers (HPC and LPC). The inside diameter of the tube is 57 mm and its total length is 3060 mm. The thermostat takes the form of a closed hydrodynamic system. The upper horizontal tube of the system (of internal diameter 200 mm) contains the shock tube with piezoelectric pressure transducers [2], and the parallel lower tube (internal diameter 120 mm) comprises an immersed pump [16], a regulating heater [11], a cooler [13], and a regulating platinum resistance thermometer [9]. Distilled water was used as the thermostatic liquid circulating in the system. Good flow mixing is ensured by the high turbulence of the flow in the gap between the shock tube and the internal surface of the thermostat. The flow velocity in this gap can be smoothly controlled. Those parts of the set-up that are in direct contact with the liquid are made of stainless steel. The temperature control of the system was achieved by a bridge arrangement: the platinum resistance thermometer [9] is connected to the arms of an R329 bridge [19]. When the temperature deviates from the prescribed value, the out-of-balance signal from the bridge is fed through an amplifier [18] to a PSR1-03 potentiometer [17], which automatically triggers the regulating heater [11]. Cooling liquid from a constant-pressure tank [10] is continuously fed into the cooler [13]. Its flow rate at a temperature in the system of 302·02 K is 20 drops per minute. This system of temperature control ensures reliable maintenance of the temperature accurate to ±0·001 K for a long period of time (more than 20 h). The total volume of the thermostat is 140 l.

The temperature in the thermostat was measured with a PTS-10 reference platinum resistance thermometer [1]. The measurement system also includes an R348 potentiometer and an R321 reference coil of 10 Ω resistance. The accuracy of the temperature measurement is 0·01 K.

To calculate the heat transfer from the outer surface of the system a theoretically possible temperature drop ΔT along the length L of the tube was determined. In the case of a non-insulated outer wall of the system the calculated value was $\Delta T/L = 3 \times 10^{-5}$ K/m. In the actual set-up the outer surface of the system was insulated by a layer of asbestos and felt of total thickness 50 mm. Consequently, the resistance thermometer [1], with a sensitivity of 0·0001 K, does not in practice detect any temperature variation in the length $L = 3200$ mm. We can therefore draw the conclusion that $\Delta T/L < 3 \times 10^{-5}$ K/m, so that the test section is isothermal.

To observe the behaviour of the interface, the test section of the shock tube has optical windows [3]. The state of the substance under near-critical conditions and the motion of the interface were visualized using a KM-6 cathetometer [15]. As illumination source [12] a filament lamp with a matt glass screen [14] was used. The lamp was switched on only for measurements, and its intensity and distance from the windows were chosen so that the heat flux from the lamp could be neglected. The error in interface measurements is 0·01 mm. Static pressure was measured with a specially calibrated MP-60 type 0·05 deadweight piston manometer [8] with an oil tank [7].

The pressure-measurement system also contains a membrane zero-indicator [4] and a microammeter [6]. The operating principle of the zero indicator is based on the triggering of an electric circuit at the moment when the pressures are equal in the cavities above and below the membrane. The pressure of the working substance below the membrane is balanced by the pressure in a nitrogen reservoir, which is measured by an MP-60 manometer. The moment of triggering is detected by the microammeter [6]. The membrane is impermeable to gases. The sensitivity of the membrane zero-indicator is 20 Pa. The membrane zero-indicator [4] and valve [5] are enclosed in the thermostat to eliminate the temperature gradient along the feedline to the shock tube. When the shock tube has been filled with the test substance the valve [5] is closed to prevent any heat transfer through the supply lines.

When the shock tube has been evacuated to 1·33 Pa using a BN-2MG pump it is filled with the substance from a pneumohydraulic system at 293·15 K. The error in the determination of the initial mass of substance in the tube was 0·093 %. The temperature in the thermostat was subsequently raised at a rate of 0·03 K/h, thus ensuring a state of quasiequilibrium of the substance in the shock tube at each moment of time.

The fundamental result has been to obtain in the set-up the critical state of trifluorochloromethane ($CCLF_3$, Freon-13). The critical parameters of F-13 were obtained with the above experimental errors: pressure (abs), $P_c = 3{\cdot}968$ MPa, temperature $T_c = 302{\cdot}02$ K, density $\rho_c = 0{\cdot}58$ g/cm^3. The results obtained are in good agreement with the scanty data of other authors, e.g. Shavandrin & Li (1979).

The regular behaviour of the substance in the critical region, earlier observed by Green (1971), such as the disappearance of the meniscus, stratification of the interface, critical opalescence, was also found in the present installation for F-13. The mass of substance transformed into the critical state was 4·526 kg.

We feel that the behaviour of the substance as it approaches the critical liquid–vapour point is interesting. As an example we describe the behaviour of the substance at an initial density $\rho_0 < \rho_c$ ($\rho_0 = 0{\cdot}576$ g/cm^3). The rate of heating was 0·03 K/h. It should be noted that at a rate of heating greater than 0·03 K/h the behaviour of the substance in the tube is quite different and there are no peculiarities in the complete light scattering and in the change in phase colouring that takes place.

The observations were made in transmitted light. At a temperature of 293·15 K the whole contents of the tube were transparent and the interface between liquid and vapour was a dark line of thickness 0·23 mm. At a height of 0·12 mm above this line there was a dark line of thickness 0·02 mm representing the meniscus. During the heating the thickness of the interface decreases and the meniscus and the interface approach each other (the surface tension tends to zero). We note that at densities $\rho_0 < \rho_c$ the interface moves downwards during the heating whereas for $\rho_0 > \rho_c$ it moves upwards. At a temperature of 301·65 K the liquid phase turns yellow, and at increasing temperatures the colour darkens, turning dark cherry close to the interface, with the vapour phase being yellowish in colour.

At $T = 301{\cdot}5$ K the interface degenerates into a dark zone of about 1·5 mm thickness in which the light absorption is a maximum. The liquid phase is then yellowish-red in colour. At a temperature of 302 K the interface becomes lighter and a thin zone appears, which at 302·02 K can be seen to stratify, and after 10 h at that temperature all the visible substance has a uniform yellowish colour. When the temperature is decreased, changes in the substance differ from those when the temperature is increased. In particular, when the density is exactly equal to its critical value, light is completely absorbed throughout the volume. At $T = 301{\cdot}51$ K and $\rho_0 = 0{\cdot}576$ g/cm^3 flying clusters of small spheres can be seen in both the liquid and the vapour. Apparently, this phenomenon corresponds to the substance being in disequilibrium.

The bursting of the diaphragm separating the HPC and LPC was initiated by two methods. In the first method, the HPC and LPC were filled with a substance at a temperature $T_0 = 293{\cdot}15$ K, with $\rho_{\mathrm{HLC}} = \rho_{\mathrm{LPC}} = \rho_c$. Then the critical parameters T_c, P_c were obtained. Immediately before the bursting, the valve of the LPC opened and the substance from this chamber entered the reservoir precooled to 78·15 K. The decrease of quantity of the substance resulted in a pressure decrease, and at a definite pressure difference between the HPC and LPC, the diaphragm burst spontaneously. The bursting pressure was varied by varying the diaphragm material.

In the second method, the LPC was filled with an amount of a substance, $\rho_{\mathrm{LPC}} < \rho_{\mathrm{HLC}} = \rho_c$, such that at $T = T_c$ the pressure drop at the diaphragm was equal to that prescribed. Then the diaphragm was cut with a knife connected to an electromagnetic device. The second method improved the repeatability of experiments and allowed the synchronization of the bursting diaphragm with the start of a high-speed camera. A rarefaction wave propagates into the high-pressure chamber. Its structure was measured by the piezoelectric pressure transducers [2], which have a flat frequency response above 50 kHz. To match the high-resistance output of the piezo-transducer with the low-resistance input of the oscilloscope a cathode follower with a pass band of 10 MHz was incorporated between them. The transducer signals were fed to the C8-11 oscilloscopes and photographed. After the firing all the substance was collected in the exhaust tank and the diaphragm was changed. The average time for one experiment was $2\frac{1}{2}$–3 days.

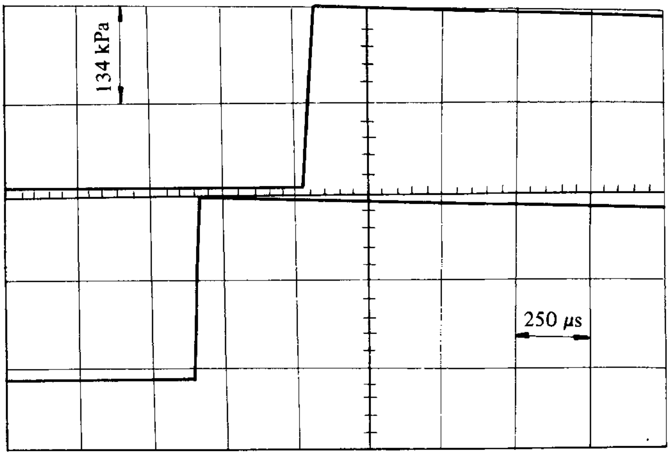

FIGURE 2. Structure of compression waves in nitrogen at $p_0 = 1$ MPa, $p_4 = 2{\cdot}35$ MPa. Lower and upper lines correspond to transducer distances from the diaphragm of 0·3 and 0·45 m respectively.

3. Experimental results

The apparatus described above was used to calibrate the pressure transducers for the cases when the unperturbed pressure P_0 ahead of the compression or rarefaction wave was significantly above atmospheric pressure ($P_0 = 0{\cdot}1$–4 MPa). For a pressure discontinuity $\Delta P = P_4 - P_0 = 0{\cdot}1$–5 MPa, where P_4 is the pressure in the high-pressure chamber, studies of compression waves in nitrogen at high initial pressures showed that, firstly, a shock wave is formed from the compression waves only for values of the parameter $\beta = \Delta P/P_0 \geqslant 0{\cdot}6$, and, secondly, that for $\beta < 0{\cdot}6$ the compression waves behave as simple waves 'decaying' with time. The shock wave formed for $\beta > 0{\cdot}6$ is shown in figure 2.

The experiments performed here for the first time demonstrated the existence of shocks that are non-broadening rarefaction waves in a substance in near-critical conditions. On figures 3(*a*, *b*) is illustrated the structure of rarefaction waves in Freon-13. Traces in figure 3(*a*) were triggered simultaneously. In figure 3(*b*) the triggering of trace 4 with respect to trace 3 was done with a time delay of $3{\cdot}8 \times 10^{-2}$ s. Then from the oscillograms 3(*a*, *b*) the velocity of the rarefaction shock wave is 50 m/s. The thickness of the rarefaction shock wave is $50 \times 0{\cdot}675 \times 10^{-3}$ m. The value of the thickness is in agreement with theoretical estimations given below. The initial parameters of the substance in front of the rarefaction wave were chosen near the thermodynamical critical point of F-13. From the oscillogram it can be seen that the rarefaction wave propagates as a surface of sudden sharp change in pressure followed by a gradual change.

In the theory of nonlinear waves (Whitham 1974) a steady state of a shock wave is characterized by the time $\tau = \Delta P/(dp/dt)_{\max}$, where ΔP is the amplitude and $(dp/dt)_{\max}$, the maximum wave steepness. This time must be short compared with the characteristic propagation time t_p of a wave in a shock tube. In our case the ratio τ/t_p is really small and is $1{\cdot}35 \times 10^{-2}$. The values of Δp and $(dp/dt)_{\max}$ for the wave profiles shown in figures 3(*a*, *b*) were determined by numerical differentiation of the curves $P(t)$.

In the wave-propagation process the time τ remained unchanged and was $6{\cdot}75 \times 10^{-4}$ s. In addition, during the experiments it was also established that the

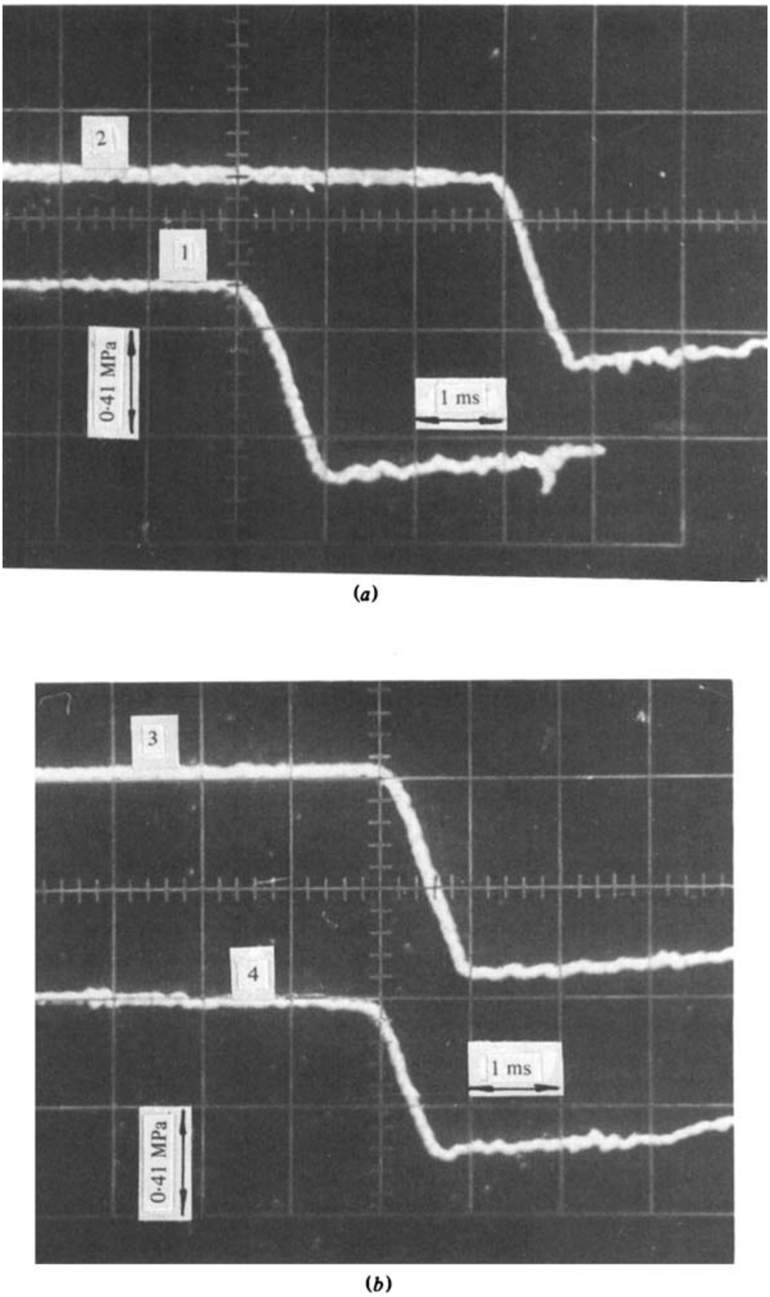

FIGURE 3. Evolution of rarefaction shock wave in Freon-13 near the critical point. Lines 1, 2, 3, 4 correspond to transducer distances from the diaphragm of 0·15, 0·30, 0·45, 2·35 m respectively.

steepness of the rarefaction wave had hardly changed after travelling a distance more than ten times its initial width, i.e. the steepness remains constant throughout the high-pressure chamber. In these experiments the initial state of the substance in the negative shock was always in a single-phase region near the critical point.

Thus our experiment clearly demonstrates that the observed phenomenon is the

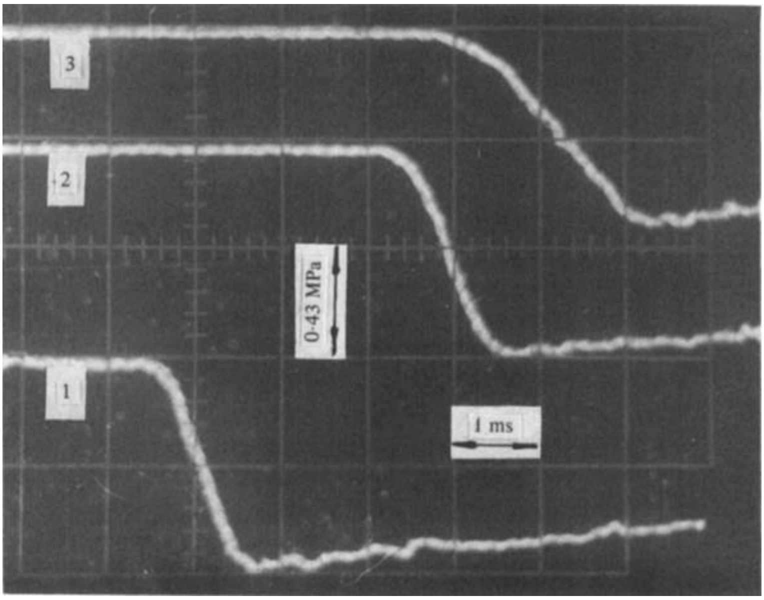

FIGURE 4. Structure of rarefaction shock wave in F-13. $p_0 = 3{\cdot}30$ MPa, $\rho_0 = 270$ kg/m³, $T_0 = 295{\cdot}15$ K. Lines 1, 2, 3 correspond to transducer distances from diaphragm of 0·15, 0·45, 2·35 m respectively.

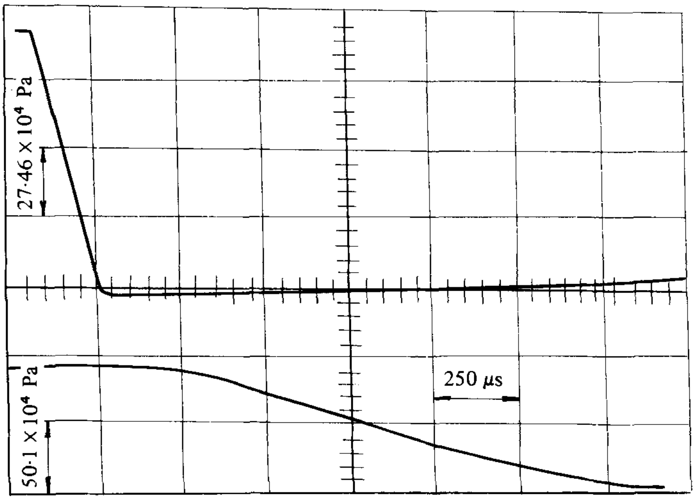

FIGURE 5. Evolution of rarefaction wave in nitrogen at $p_0 = 3{\cdot}88$ MPa, $T_0 = 301{\cdot}54$ K. Upper and lower lines correspond to transducer distances of 0·45 and 2·35 m respectively.

rarefaction shock or negative shock, defined by Zeldovich (1946) as a surface of sudden very sharp change in the properties of the substance that propagates relative to the unperturbed substance.

To confirm that the negative shock only exists in the critical region, an experiment was performed on the evolution of rarefaction in F-13 and in nitrogen. Far from the critical point the initial parameters ahead of the wave were chosen as $T/T_c = 0{\cdot}98$, $P/P_c = 0{\cdot}83$, $\rho/\rho_c = 0{\cdot}465$ for Freon-13 (figure 4); and $T/T_c = 2{\cdot}39$, $P/P_c = 1{\cdot}14$,

$\rho/\rho_c = 0{\cdot}145$ for nitrogen (figure 5). As expected, in none of the experiments with nitrogen did a negative shock wave develop. During the evolution of the rarefaction wave it spread so that over the same distance its steepness was reduced by a factor of five or more.

Experiments performed at different times gave good agreement of all oscilloscope records. The errors in the measurement of the dynamic characteristics using the piezoelectric transducers were 1 % for the wave velocities and less than 12 % for the pressure amplitudes.

4. Theory of the evolution of finite perturbations close to the critical liquid–vapour point

As is well known (Green 1971), in close proximity to the thermodynamic critical point, compressibility, heat capacity and kinetic coefficients become abnormally high, and tend to infinity when the thermodynamic variables are exactly at the critical point. Under conditions near to the critical state the medium becomes very sensitive to external thermal or dynamic perturbations, and the anomalies in turn have a strong effect on the structure of these perturbations.

Consider the propagation of finite perturbations of pressure, density or particle velocity in a medium whose initial state is close to the critical point. The perturbations are assumed to be long-wave, i.e. the correlation radius is much smaller than their characteristic length. In this case the contribution from relaxation processes is significantly smaller than that of dissipation.

The complete system of equations describing the motion of the medium close to the critical point has, in the hydrodynamic approximation, the form

$$\rho[\mathbf{v}_t+(\mathbf{v}\,.\,\nabla)\,\mathbf{v}] = -\nabla P+\eta\nabla^2\mathbf{v}+(\xi+\tfrac{1}{3}\eta)\,\nabla(\nabla\,.\,\mathbf{v}),$$

$$\rho T[S_t+\mathbf{v}\,.\,\nabla S] = \kappa\nabla^2 T+\xi(\nabla\,.\,\mathbf{v})^2+\tfrac{1}{2}\eta\left(\frac{\partial \mathbf{v}_i}{\partial x_k}+\frac{\partial \mathbf{v}_k}{\partial x_i}-\tfrac{2}{3}\delta_{ik}\frac{\partial \mathbf{v}_l}{\partial x_l}\right)^2,$$

$$P = P(\rho,S),\quad \rho_t+\partial\,.\,(\rho\mathbf{v}) = 0,$$

where S is the entropy, P the pressure, ρ the density, and $\mathbf{v}$ is the velocity of the medium in laboratory coordinates (x,t). Suffixes x and t indicate partial derivatives; ξ and η are the bulk and shear viscosities and κ is the coefficient of thermal conductivity.

We assume that the relative deviations $(P-P_0)/P_0$, $(\rho-\rho_0)/\rho_0$ and $(|\mathbf{v}|-|\mathbf{v}_0|)/C_0$ (P_0, r_0, and $|\mathbf{v}_0|$ are the equilibrium values, and C_0 is the speed of sound) are caused by a wave whose amplitude is small to first order μ. Besides, we assume the dissipative effects to be also small, i.e. ξ, η, $K \sim \mu$. Neglecting in the original system of equations the terms exceeding the second order of smallness, we reduce it to the form

$$(\rho'+\rho_0)\frac{\partial \mathbf{v}}{\partial t} = -\nabla p'+(\xi+\tfrac{1}{3}\eta)\,\nabla(\nabla\,.\,\mathbf{v}')-\rho_0(\mathbf{v}'\,.\,\nabla)\,\mathbf{v}',$$

$$\rho_0 T_0\frac{\partial S'}{\partial t} = K\nabla^2 T',$$

$$\frac{\partial \rho'}{\partial t}+\rho_0\nabla\,.\,\mathbf{v}' = 0,$$

$$P' = \left(\frac{\partial P}{\partial \rho}\right)_S\rho'+\frac{1}{2}\left(\frac{\partial^2 P}{\partial \rho^2}\right)_S\rho'^2+\left(\frac{\partial P}{\partial S}\right)_\rho S'.$$

By putting in the question for entropy $T' = P'(\partial T/\partial P)_S$ we obtain

$$\rho_0 T_0 \frac{\partial S'}{\partial t} = K\left(\frac{\partial T}{\partial P}\right)_S \nabla^2 P'.$$

From the equation of motion we have

$$\rho_0 \frac{\partial}{\partial t}\nabla . \mathbf{v}' = -\nabla . (\nabla P') + \frac{\partial}{\partial t} O(\mu^2),$$

Taking into account that $\nabla . (\nabla P') = \nabla^2 P'$,

we obtain
$$\rho_0 T_0 \frac{\partial S'}{\partial t} = -K\left(\frac{\partial T}{\partial P}\right)_S \rho_0\left[\frac{\partial}{\partial t}\nabla . \mathbf{v}' + \frac{\partial}{\partial t} O(\mu^2)\right].$$

Taking into account the fact that the dissipation due to heat conduction, i.e. $kO(\mu^2) = O(\mu^3)$, we obtain

$$S' = -\frac{K}{T_0}\left(\frac{\partial T}{\partial P}\right)_S \nabla . \mathbf{v}'.$$

Then the equation of state takes the form

$$P' = C_0^2 \rho' - \frac{K}{T_0}\left(\frac{\partial P}{\partial S}\right)_\rho \left(\frac{\partial T}{\partial P}\right)_S \nabla . \mathbf{v}' + \frac{1}{2}\left(\frac{\partial^2 P}{\partial \rho^2}\right)_S \rho'^2, \tag{1}$$

where
$$C_0^2 = \left(\frac{\partial P}{\partial \rho}\right)_S; \quad P' = P - P_0, \quad \rho' = \rho - \rho_0, \quad \mathbf{v} = \mathbf{v} - \mathbf{v}_0, \quad \mathbf{v}_0 = 0.$$

Further we shall consider only the propagation of plane waves, since in a shock tube this case has most applicability. However, we note that further conclusions will be valid for cylindrically and spherically symmetrical waves. In these cases also one equation may be obtained for one of the perturbed values.

Thus, retaining the terms of the second order of smallness in the equations of motion and continuity, and replacing the pressure using the equation of state in the equation of motion, we obtained the following system of equations for plane waves:

$$(\rho_0 + \rho')\, v'_t + \rho_0 v' v'_x = -C_0^2 \rho'_x - \left(\frac{\partial^2 P}{\partial \rho^2}\right)_S \rho' \rho'_x + b v'_{xx}, \tag{2}$$

$$\rho'_t + (\rho_0 + \rho')\, v'_x + v \rho'_x = 0, \tag{3}$$

where
$$b = \xi + \tfrac{4}{3}\eta + \frac{\kappa}{T_0}\left(\frac{\partial P}{\partial S}\right)_\rho \left(\frac{\partial T}{\partial P}\right)_S,$$

By differentiating (2) with respect to x, and (3) with resect to t, then eliminating v'_{xt} from the resulting equations using substitutions $v' = C_0 \rho'/\rho_0$, $\rho'_t = -\rho_0 v'_x$ in the terms of the second order of smallness, we obtain a hyperbolic wave equation for ρ':

$$C_0^2 \rho'_{xx} + \frac{2C_0^2}{\rho_0}\left[1 + \frac{\rho_0}{2C_0^2}\left(\frac{\partial^2 P}{\partial \rho^2}\right)_S\right](\rho' \rho'_x)_x = \rho'_{tt} + \frac{bC_0}{\rho_0}\rho'_{xxx}.$$

This equation describes the propagation of nonlinear waves in both directions. We will not consider further the interaction region of waves propagating to the right and to the left, but will treat only the evolution of a single rarefaction wave forming after the bursting of the diaphragm and spreading through the HPC.

Considering a perturbation which propagates in the positive x-direction we find the solution to the last system of equations, again to second order, using the method of Khokhlov (1961). Because of the weak nonlinearity of the process under consideration, the perturbations v' and ρ' can be represented as slowly varying functions of coordinates, so that v' and $\rho' = F(\mu x, t-x/C_0)$. This means that the perturbations change their shape only slowly as they evolve in the x-direction.

In this case (2) and (3) in the variables $z = \mu x$, $\tau = t-x/C_0$ take the form

$$\mu C_0^2\frac{\partial\rho'}{\partial x}-C_0\frac{\partial\rho'}{\partial\tau}+(\rho_0+\rho')\frac{\partial v'}{\partial\tau}-\frac{\rho_0}{C_0}v'\frac{\partial v'}{\partial\tau}-\left(\frac{\partial^2P}{\partial\rho^2}\right)_S\frac{\rho'}{C_0^2}\frac{\partial\rho'}{\partial\tau}=-\frac{b}{C_0^2}\frac{\partial^2v'}{\partial\tau^2},$$

$$\mu\rho_0\frac{\partial v'}{\partial x}+\frac{\partial\rho'}{\partial\tau}\left(1-\frac{v'}{C_0}\right)-\frac{1}{C_0}(\rho_0+\rho')\frac{\partial v'}{\partial\tau}=0.$$

The equations describing the evolution of v', ρ' must be of similar form, since they are characteristics of a single-wave process. This means that, in the nonlinear case, the linear relation $v' = \rho' C_0/\rho_0$ must be complemented by terms of the second order of smallness and by some derivatives with unknown coefficients a and d such that $a \sim 1$, $d \sim O(\mu)$, and

$$\rho' = \frac{\rho_0}{C_0}v'+\frac{a\rho_0}{C_0}v'^2+\frac{d\rho_0}{C_0}\frac{\partial v'}{\partial\tau},$$

$$v' = \frac{C_0}{\rho_0}\rho'-\frac{aC_0^2}{\rho_0^2}\rho'^2-\frac{dC_0}{\rho_0}\frac{\partial\rho'}{\partial\tau}.$$

By substituting now the perturbation of the velocity v' as a function of density, i.e. $v' = f_1(\rho')$ into the equation of motion, and $\rho' = f_2(v')$ into the equation of continuity, we get

$$\mu\frac{C_0}{\rho_0}\frac{\partial\rho'}{\partial x}-2\frac{\rho'}{\rho_0^2}\frac{\partial\rho'}{\partial\tau}\left[aC_0+\left(\frac{\partial^2P}{\partial\rho^2}\right)_S\frac{\rho_0}{2C_0^2}\right]=\left[\frac{b}{C_0^2\rho_0}+d\right]\frac{1}{\rho_0}\frac{\partial^2\rho'}{\partial\tau^2},$$

$$\mu\frac{\partial v'}{\partial x}-2\frac{v'}{C_0^2}\frac{\partial v'}{\partial\tau}[1-aC_0]=-\frac{d}{C_0}\frac{\partial^2v'}{\partial\tau^2}.$$

From a comparison of coefficients of the nonlinear and dissipative terms the constants a and d are determined:

$$a=\frac{1}{2C_0}-\left(\frac{\partial^2P}{\partial\rho^2}\right)_S\frac{\rho_0}{4C_0^3},\quad d=-\frac{b}{2\rho_0C_0^2}.$$

Substituting a and d into the equation for the velocity perturbation, we obtain

$$\mu v'_x-\left[1+\frac{\rho}{2C_0^2}\left(\frac{\partial^2P}{\partial\rho^2}\right)_S\right]\frac{v'}{C_0^2}v'_\tau=\frac{b}{2\rho_0C_0^3}v'_{\tau\tau}. \tag{4}$$

Thus we have obtained the Burgers equation written in a coordinate system moving with velocity C_0. The equations for the perturbations p' and ρ' are obtained from (4) by replacing v' by P'/ρ_0C_0 and $C_0\rho'/\rho_0$ respectively. For ideal gases the expression in square brackets is simply $\frac{1}{2}(\gamma+1)$. For real gases, however, the second derivative near the critical point has the abnormal condition $(\partial^2P/\partial\rho^2)_S < 0$, and the overall expression in the brackets may become negative. In this case (4) describes the evolution of a rarefaction shock wave. In fact, in the laboratory system of coordinates, the equation (4) for the pressure can be rewritten as

$$P'_t+C_0P'_x+\frac{1}{2\rho_0^3C_0^2}\left(\frac{\partial^2P}{\partial V^2}\right)_S\frac{P'P'_x}{\rho_0C_0}=\frac{1}{2\rho_0}\left[\tfrac{4}{3}\eta+\xi+\kappa\left(\frac{1}{c_v}-\frac{1}{c_p}\right)\right]P'_{xx}, \tag{5}$$

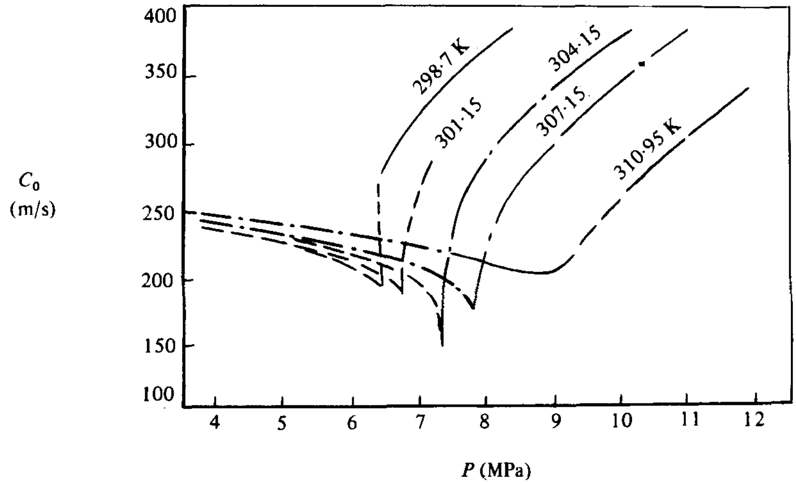

FIGURE 6. Sound speed in carbon dioxide versus pressure near the critical point according to Tielsch & Tanneberger (1954).

where V is the specific volume and c_v and c_p the specific heats at constant volume and pressure respectively. The factor in the nonlinear term in (5) can be written as

$$\alpha = \frac{1}{2\rho_0^3 C_0^2}\left(\frac{\partial^2 P}{\partial V^2}\right)_S = 1 + \frac{\rho_0}{2C_0^2}\left(\frac{\partial^2 P}{\partial \rho^2}\right)_S = 1 + \rho_0 C_0\left(\frac{\partial C_0}{\partial P}\right)_S,$$

from which it follows that the change in sign of α is associated with the abnormal decrease in the speed of sound when the pressure increases near the critical point (figure 6). From (5) it is easy to obtain the velocity of a pressure jump with amplitude P':

$$D(P') = C_0 + \tfrac{1}{2}P'\left[\left(\frac{\partial C_0}{\partial P}\right)_S + \frac{1}{\rho_0 C_0}\right]. \tag{6}$$

It can be seen from figure 6 that in a rarefaction wave $(\partial C_0/\partial P)_S < 0$ near the critical point, and quickly attains that negative value at which the expression in the square bracket in (6) also becomes negative. Hence $P'[(\partial C_0/\partial P)_S + 1/\rho_0 C_0] > 0$, so that the velocity at each point of the wave profile increases when the modulus of the pressure increases. This leads to the formation of a discontinuity in the rarefaction wave, i.e. a negative shock wave. A similar effect for the temperature jumps in superconducting fluids was reported by Khalatnikov (1971). Furthermore, the velocity of the pressure jump satisfies the condition for mechanical stability $C_0 < D < C_1 - v$. In fact, if we substitute the values of the speed of sound in the disturbed medium C_1 and the particle velocity v' we get

$$C_0 < D < C_0 + P'\left[\left(\frac{\partial C_0}{\partial P}\right)_S + \frac{1}{\rho_0 C_0}\right].$$

In this case the entropy condition (Zeldovich 1946),

$$S_1 - S_0 = \frac{1}{12T_0}\left(\frac{\partial^2 P}{\partial V^2}\right)_S (v_0 - v_1)^3,$$

is satisfied automatically since $(\partial^2 P/\partial V^2)_S < 0$ for the same range of parameters as the coefficient $[(\partial C_0/\partial P)_S + 1/\rho_0 C_0]$ in the condition for mechanical stability.

The factor in the second derivative in (5) takes abnormally high values close to the critical point, and may be evaluated by one of the known models (Green 1971). Let us estimate the width of the transition zone, i.e. the 'thickness' δ of a rarefaction shock wave. Its value is determined by

$$\delta = \frac{bC_0}{P' \dfrac{1}{2\rho_0^3 C_0^2}\left(\dfrac{\partial^2 P}{\partial V^2}\right)_S}. \tag{7}$$

By means of the theory of interacting modes, Kadanoff & Swift (1968) determined the damping factor

$$\beta = b\pi\omega / C_0^2 \rho,$$

which near the critical point behaves as

$$\beta = \omega\epsilon^{-2},$$

where $\epsilon = |T - T_c| / T_c$.

Such a formula for β is valid for values $\omega\epsilon^{-2} < 5 \times 10^{-3}$. In our case this inequality is fulfilled. Let us estimate now the nonlinearity coefficient using Bethe's formula (Lambrakis & Thompson 1972):

$$\left(\frac{\partial^2 P}{\partial V^2}\right)_S = \left(\frac{\partial^2 P}{\partial V^2}\right)_T - \frac{3T}{C_v}\left(\frac{\partial P}{\partial T}\right)_v \frac{\partial^2 P}{\partial V \partial T} + \frac{3T}{C_v^2}\left(\frac{\partial P}{\partial T}\right)^2 \left(\frac{\partial^2 P}{\partial T^2}\right)_v + \frac{T}{C_v^2}\left(\frac{\partial P}{\partial T}\right)_v^3 \left\{1 - \frac{T}{C_v}\left(\frac{\partial C_v}{\partial T}\right)_v\right\}.$$

It is seen that, when the critical point is approached, the first term on the right-hand side goes to zero according to the definition, the second term also goes to zero, the third one tends to zero as $\epsilon^{2\bar{\alpha}}$, where $\bar{\alpha} \approx 0{\cdot}1$ is the exponent of specific heat singularity at constant volume $C_v \sim |T - T_c|^{-\bar{\alpha}}$, T_c being the critical temperature. The last term increases as $T \rightarrow T_c$ as $\epsilon^{-1+2\bar{\alpha}}$. Thus the coefficient

$$\alpha = \frac{V^3}{2C_0^2}\left(\frac{\partial^2 P}{\partial V^2}\right)_S = \epsilon^{-1+2\bar{\alpha}}\epsilon^{-\bar{\alpha}} = \epsilon^{-1+\bar{\alpha}},$$

and

$$\delta = \delta_0 \left|\frac{T - T_c}{T_c}\right|^{-1-\frac{1}{2}\bar{\alpha}},$$

where δ_0 is a value independent of the temperature difference $T - T_c$ having the meaning of the transition-zone width of a compression shock wave far from the critical point. The value of δ_0 is $\approx 0{\cdot}88 \times 10^{-7}$ m, i.e. of the order of several mean free paths. For the case realized in our experiments, where $T - T_c = 10^{-3}$, we obtain $|T - T_c|/T_c = 3 \times 10^{-6}$, $\delta/\delta_0 = 629540$, from whence

$$\delta = 0{\cdot}88 \times 10^{-5} \times 629540 = 5{\cdot}6 \text{ cm}.$$

Thus the transient-zone width of the rarefaction shock wave close to the critical point is determined not by the mean free path of molecules but by the other scale, which exceeds the mean free path by a large factor. Close to the critical point, indeed, a new internal scale appears, a correlation radius, which also increases infinitely at $T \rightarrow T_c$. The correlation radius here seems to be a determining scale also for the width of the rarefaction shock wave.

Equation (5) has a solution describing a stationary shock wave (Rudenko & Soluyan 1974):

$$P = P_0 + \frac{\Delta P}{1 + \exp(\epsilon\alpha\Delta P / bC)},$$

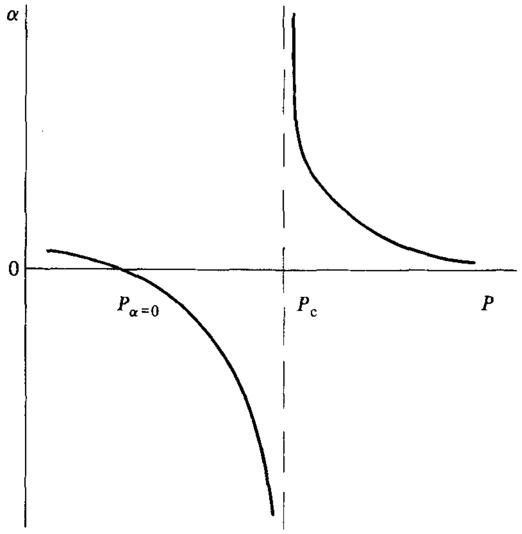

FIGURE 7. Factor α in the nonlinear term in (5) versus pressure on the critical isotherm.

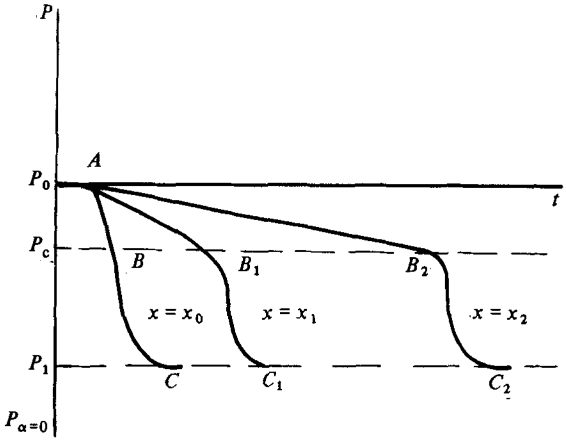

FIGURE 8. Splitting of rarefaction wave into centred and shock rarefaction waves ($x_2 > x_1 > x_0$).

where
$$\Delta P = P_{\xi=-\infty} - P_{\xi=+\infty}, \quad \xi = x - Dt, \quad \left.\frac{\partial P}{\partial \xi}\right|_{\xi=\pm\infty} = 0.$$

It is seen from the solution that if α is negative there exists a stationary solution in the form of a rarefaction shock wave. In the case $\alpha > 0$ no stationary solutions exist in the form of a rarefaction shock wave; rarefaction waves decay away in the process of evolution. The coefficient α changes its sign when the pressure decreases when the medium in the unperturbed state is at a pressure $P_0 > P_c$ (figure 7). In this case the rarefaction wave *ABC* will split into two parts: the first (AB_1) will be centred with a decaying front, and the second ($B_1 C_1$) will be abnormal, corresponding to a negative shock (figure 8). In the case $P_{\alpha=0} < P_0 < P_c$ and $P_1 < P_{\alpha=0}$, where P_1 is the pressure in the final state (figure 9) the wave splits into a negative shock AB_1 and a simple

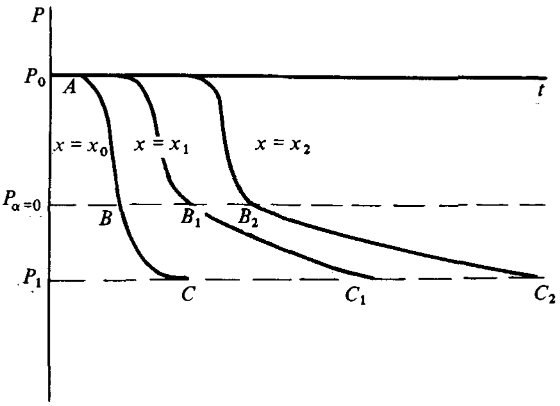

FIGURE 9. Splitting of rarefaction wave into shock and simple decaying-front waves ($x_2 > x_1 > x_0$).

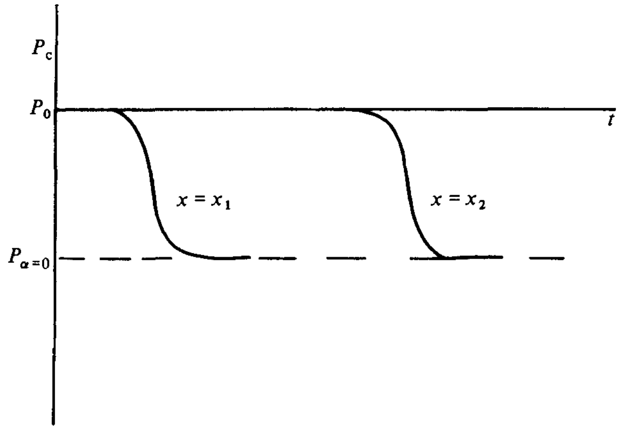

FIGURE 10. Shock rarefaction wave ($x_2 > x_1$).

wave B_1C_1 with a decaying front. Analogous pressure profiles will be observed if a first-order phase transition takes place in the wave near the critical point, since the vapour and liquid properties here are similar and the main contribution to the wave structure is the difference between the speeds of sound in the liquid and gas phases. The wave evolution in this case is also described by (5). Hence, the structure of rarefaction waves (figures 8 and 9) depends greatly on the values of the parameters of the unperturbed and final states relative to the critical point, and can be qualitatively interpreted using figures 6 and 7. Equation (5) with a constant factor in the nonlinear term has been analysed by several authors. Note that taking account of the dependence of this factor on the pressure provides the results illustrated in figures 8 and 9. From figures 7 and 10 it can be seen that the negative shock wave exists as a single structure if its pressure satisfies the condition $P_{\alpha=0} \leqslant P \leqslant P_c$. Otherwise it splits up. (Thus if $P_0 > P_c$ but $P_1 < P_{\alpha=0}$, the wave profile may consist of three parts.)

Thus the propagation of long-wave perturbations near the critical point is described by (5), which gives the solution in the form of negative shock waves and accounts for the multiwave structure of rarefaction waves in the critical region.

5. Conclusions

For the first time the existence of a new phenomenon, the rarefaction shock wave or negative shock wave, has been demonstrated experimentally. This phenomenon has been discovered in the single-phase region and its origin is not due to phase transitions. Its existence is attributed to the abnormal decrease in the speed of sound near the critical point when the pressure increases. The decrease in the speed of sound is in turn associated with the abnormal increase in the heat capacity and compressibility in the critical region owing to the strong interaction of the constituent molecules of the substance.

The evolution of finite-amplitude perturbations near the critical point has been described theoretically. The condition for the formation of a shock wave obtained from the evolution equation is in precise agreement with the similar criterion obtained by Zeldovich from the entropy condition for shock-wave stability.

The negative shock wave may be a new and simpler effective tool for the study of the abnormal behaviour of the heat capacity, compressibility, and kinetic coefficients of substances in the critical liquid–vapour region.

The application of the negative shock wave will allow us to develop a dynamical method for the study of critical phenomena.

REFERENCES

GREEN, M. S. (ed.) 1971 *Critical Phenomena. Proc. Int. School of Physics 'Enrico Fermi', Course* LI. Academic.

KADANOFF, L. P. & SWIFT, J. 1968 Transport coefficients near the liquid–gas critical point. *Phys. Rev.* **166**, 89–101.

KHALATNIKOV, I. M. 1971 *Theory of Superfluids.* Nauka.

KHOKHLOV, R. V. 1961 Theory of shock radio waves in nonlinear lines. *Radiotekhnika i Electronika* **6**, 917–925.

KUTATELADZE, S. S., BORISOV, AL. A., BORISOV, A. A. & NAKORYAKOV, V. E. 1980 Experimental detection of a shock rarefaction wave near the critical point liquid–vapour. *Dokl. Akad. Nauk SSSR* **252**, 595–598.

LAMBRAKIS, K. C. & THOMPSON, P. A. 1972 Existence of real fluids with a negative fundamental derivative Γ. *Phys. Fluids* **15**, 933–935.

RUDENKO, O.V. & SOLUYAN, S. I. 1974 Theoretical foundations of nonlinear acoustics. Nauka. (English translation 1977 by Consultants Bureau, New York.)

SHAVANDRIN, A. M. & LI, S. A. 1979 Experimental studies of temperature–density parameters under F-13 saturation. *Inzh. Fiz. Zh.* **37**, 830–834.

THOMPSON, P. A. & LAMBRAKIS, K. C. 1973 Negative shock waves. *J. Fluid Mech.* **60**, 187–208.

TIELSCH, H. & TANNEBERGER, H. 1954 Ultraschallausbreitung in Kohlensäure in der Nähe des kritischen Punktes. *Z. Phys.* **137**, 256–264.

WHITHAM, G. B. 1974 *Linear and Nonlinear Waves.* Wiley.

ZELDOVICH, YA. B. 1946 The possibility of shock rarefaction waves. *Zh. Eksp. Teor. Fiz.* **16**, 363–364.